Flexible terahertz metamaterials for dual-axis strain sensing

Jining Li,[1,2] Charan M. Shah,[3] Withawat Withayachumnankul,[1,3,*] Benjamin S.-Y. Ung,[1] Arnan Mitchell,[3] Sharath Sriram,[3] Madhu Bhaskaran,[3,4] Shengjiang Chang,[2] and Derek Abbott[1]

[1]*School of Electrical and Electronic Engineering, The University of Adelaide, Adelaide SA 5005, Australia*

[2]*Institute of Modern Optics, Nankai University, Tianjin 300071, China*

[3]*Functional Materials and Microsystems Research Group, RMIT University, Melbourne VIC 3001, Australia*

[4]*e-mail: madhu.bhaskaran@rmit.edu.au*

**Corresponding author: withawat@eleceng.adelaide.edu.au*

Received April 15, 2013; accepted May 8, 2013;
posted May 20, 2013 (Doc. ID 188835); published June 11, 2013

Utilizing an elastic polymer, we design and experimentally demonstrate a four-fold symmetric flexible metamaterial operating at terahertz frequencies. The fabricated metamaterials exhibit good stretchability and recoverability. Two independent resonances can be observed when the structure is probed with linearly polarized terahertz waves in two orthogonal axes. Applying a stretching force along a main axis causes an observable frequency shift in the corresponding resonance, with minimal effect on the other. This study suggests a possible application of flexible metamaterials for dual-axis strain sensing.

OCIS codes: (160.3918) Metamaterials; (300.6495) Spectroscopy, terahertz.
http://dx.doi.org/10.1364/OL.38.002104

Metamaterials are artificial composites that can manipulate electromagnetic waves in unique ways [1]. They can be used to realize numerous applications, including superlenses [2], invisibility cloaks [3], perfect absorbers [4], and strain sensors [5]. By attaching a relatively small metamaterial-based strain sensor onto the surface of an object, its resonance behavior with the mechanical properties of the structure as a function of object deformation can be telemetrically measured in real time. Unlike other techniques, metamaterial-based devices do not need any form of power source to support their operation. The resonance of metamaterials can be relatively strong, leading to high sensitivity for sensing. Recently, they have been demonstrated for wireless strain sensing, particularly under a compressive force, at radio frequencies [6,7]. Scaling the structure to the terahertz regime will result in an improvement in the sample size and the spatial sensitivity owing to the relatively short wavelength of terahertz waves.

The advancement of polymer technologies and lithographic techniques makes it possible to fabricate terahertz metamaterials on thin flexible substrates, to accommodate large mechanical deformation [8]. Thin terahertz metamaterials have been fabricated on flexible polyimide substrates, which can be rolled into cylinders [9]. Metamaterials fabricated on flexible polyethylene naphthalate films realized the resonance tunability by being wrapped up into tubes with various diameters [10]. The stretchable wrinkles on polydimethylsiloxane (PDMS) substrates have been utilized to adjust the resonance frequency of terahertz metamaterials [11].

Previously, we developed mechanically tunable metamaterials based on a single I-shaped dipole design operating at terahertz frequencies [12]. The resonance frequency could be shifted and fully recovered as a function of the applied strain along the polarization axis. In this Letter, we present the design, fabrication and characterization of four-fold symmetric flexible terahertz metamaterials for dual-axis strain sensing. In the absence of substrate deformation, the structure exhibits a 2D isotropic response to the incident terahertz radiation. The applied strain along the main axis leads to optical anisotropy, which is manifested through a change in the resonance behavior. By observing this anisotropic resonance property, it is possible to distinguish the strain from the two orthogonal directions.

The unit cell shown in Figs. 1(a) and 1(b) comprises a 200 nm thick gold layer of resonators encapsulated between the 100 and 10 μm thick polymer substrate and superstrate. Each resonator is composed of two orthogonal dipoles capped with interdigitated capacitors. When a linearly polarized terahertz wave is transmitted through this metamaterial, the incident electric field induces a large accumulation of surface charges in the opposite

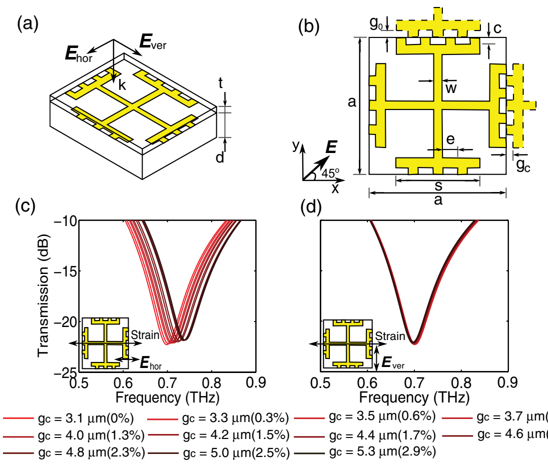

Fig. 1. (a) and (b) Schematics of the unit cell with dimensions $a = 78$ μm, $s = 47$ μm, $e = 9$ μm, $c = 3$ μm, $g_0 = 3$ μm, $g_c = 3$ μm, $w = 5$ μm, $t = 10$ μm, and $d = 100$ μm. (c) and (d) Numerical results for the transmission spectra with different gap widths, for the horizontal and vertical polarizations, respectively, when the strain is loaded along the x axis. The percentage values are the calculated strain of the unit cell.

edges of the dipole that aligns with the polarization; hence, a strong electric field is established across the capacitive gap between dipoles. The dipole resonance frequency can be approximately evaluated from the equivalent inductance and capacitance in the form of $f_0 = 1/(2\pi\sqrt{LC})$.

The substrate and superstrate are made of PDMS, which is a flexible polymer with excellent mechanical durability. The substrate and superstrate deformations result in a change in the width of the capacitive gaps perpendicular to the applied strain. The capacitive alteration results in a change in the resonance, which can be interrogated via terahertz radiation with a polarization in the direction parallel to the strain. The resonance frequency shifts toward higher frequencies with an increasing gap width, and *vice versa*. The interdigitated gaps between unit cells lead to a higher Q–factor resonance and consequently improved sensitivity [13].

To predict the electromagnetic resonance behavior of the resonators, the design is simulated by using CST Microwave Studio. The simulated transmission at the frequencies from 0.5 to 0.9 THz can be found in Figs. 1(c) and 1(d). At equilibrium, i.e., in the absence of an applied force, the resonance frequencies for the two orthogonal dipoles are equal to 0.69 THz and the Q factor calculated from $f_0/\Delta f$ is equal to 13. The stretching force applied along the horizontal axis is expected to change the width of the vertical gap from 3.1 to 5.3 μm. In this case, the simulation shows that the resonance frequency for the horizontal dipole shifts from 0.698 to 0.740 THz. Despite this, the resonance of the vertical dipole is minimally affected by this mechanical deformation.

The resonator structures are fabricated by standard microfabrication techniques that are adapted to flexible materials. The PDMS substrate layer is obtained by standard spin-coating processes on a silicon wafer. A thin film of gold is then deposited on this spin-coated PDMS layer, which rests on top of a supporting silicon wafer, by using electron beam evaporation at room temperature. During this metallization, a 20 nm thick layer of chromium is first deposited to serve as an adhesion layer below the gold layer. The resonators are then patterned onto these metal layers by using standard photolithography and etching techniques. The fabrication process is completed by spin coating and curing a final layer of PDMS on the top of the patterned sample, to protect the gold films underneath from possible damage. The completed sandwiched sample is then peeled from the supporting silicon wafer. The overall dimensions of each patterned array is approximately 10 mm × 10 mm.

The measurement is performed by using a fiber-coupled terahertz time-domain spectroscopy system. The terahertz beam is collimated and focused onto the sample by two polymer lenses. The polarization of the emitter is set to 45° with respect to the horizontal axis, with a polarizer placed in the middle of the two lenses to further refine the polarization angle. The fabricated metamaterial is mounted using two plastic clamps that are attached to a custom-made test jig, which allows the mechanical stretching with micrometer precision. The transmitted terahertz waves for the two orthogonal polarizations, E_{hor} and E_{ver}, are detected separately by adjusting another polarizer in front of the detector. The initial sample length, less the area covered by the clamps, is $l_0 = 6.14$ mm. The stretching displacement is applied in discrete steps with $\Delta l = 60$ μm defining the step size. The strain is defined as $(l - l_0)/l_0 \times 100\%$, where l is the stretched sample length. During the experiment, the strain is varied up to 10 steps. At every Δl step, the two signals with orthogonal polarizations are recorded.

The transmission responses are presented in Fig. 2. The initial resonance frequency of the metamaterial for the two orthogonal polarizations at its relaxed position is equal to 0.70 THz, which matches well with the predictions from simulation. As stretching is applied along the horizontal direction up to $10\Delta l$, the resonance frequency of the horizontal dipole shifts upward by 36 GHz, to 0.74 THz, or about 6%, as shown in Fig. 2(a). The resonance frequency for the vertical dipole remains around the initial frequency under the horizontal strain, as shown in Fig. 2(b). Figure 3 shows the resonance frequency for the horizontal dipole as a function of the applied strain. This relationship indicates a reasonably linear sensitivity level of 3.68 GHz/% strain. In addition, in Fig. 2(a) the transmission minimum for the horizontal dipole resonance increases with an increase in strain, due to a decrease in the gap capacitance. The strain in the experiment is about 3 times larger than that in the simulation. This discrepancy is due to the nonuniform local stretching in the direction of the applied force, which results in strain variation over the sample surface. Discrepancies in the transmission magnitude between the numerical and experimental results can be ascribed to the dielectric loss of PDMS and the geometric tolerances in the samples. The experimental results demonstrate that the two dipole resonances respond separately to the orthogonal stretching. The resonance changes only when the applied stretching component aligns with the respective dipole.

In this Letter, we have designed and fabricated a terahertz metamaterial on a highly flexible polymer substrate. Each resonator is made of two orthogonal dipoles capped with interdigitated capacitors. The

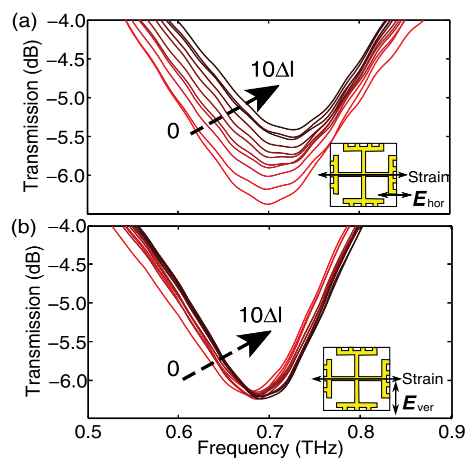

Fig. 2. Measured transmission magnitude of the fabricated metamaterials with the polarization is (a) parallel and (b) perpendicular to the applied force.

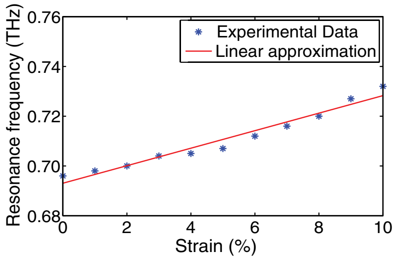

Fig. 3. Resonance frequency as a function of the applied strain. The resonance frequency is taken from Fig. 2(a).

resonance frequencies for the two dipoles in a single unit cell can be independently tuned by applying stretching strain in the respective directions. This research suggests an application of terahertz metamaterials in dual-axis strain sensing. The strain sensing for the two axes can be carried out simultaneously by designing the unit cell to resonate at different frequencies for the two orthogonal polarizations. A flexible metamaterial substrate can be employed to realize strong resonance, which leads to an improvement in the sensitivity of sensing.

J. L. acknowledges the National High Technology Research and Development Program of China (Grant No. 2011AA010205) and the National Natural Science Foundation of China (Grant No. 61171027). W. W., S. S., and M. B. acknowledge Australian Post-Doctoral Fellowships from the Australian Research Council (ARC) through Discovery Projects DP1095151, DP110100262, and DP1092717, respectively. D. A. and W. W. acknowledge funding from ARC Discovery Project DP120100200.

References

1. W. Withayachumnankul and D. Abbott, IEEE Photon. J. **1**, 99 (2009).
2. X. Zhang and Z. Liu, Nat. Mater. **7**, 435 (2008).
3. D. Schurig, J. J. Mock, B. J. Justice, S. A. Cummer, J. B. Pendry, A. F. Starr, and D. R. Smith, Science **314**, 977 (2006).
4. N. I. Landy, S. Sajuyigbe, J. J. Mock, D. R. Smith, and W. J. Padilla, Phys. Rev. Lett. **100**, 207402 (2008).
5. I. M. Pryce, K. Aydin, Y. A. Kelaita, R. M. Briggs, and H. A. Atwater, Nano Lett. **10**, 4222 (2010).
6. R. Melik, E. Unal, N. K. Perkgoz, C. Puttlitz, and H. V. Demir, Appl. Phys. Lett. **95**, 011106 (2009).
7. R. Melik, E. Unal, N. K. Perkgoz, C. Puttlitz, and H. V. Demir, Opt. Express **18**, 5000 (2010).
8. I. E. Khodasevych, C. M. Shah, S. Sriram, M. Bhaskaran, W. Withayachumnankul, B. S.-Y. Ung, H. Lin, W. S. T. Rowe, D. Abbott, and A. Mitchell, Appl. Phys. Lett. **100**, 061101 (2012).
9. H. Tao, A. C. Strikwerda, K. Fan, C. M. Bingham, W. J. Padilla, X. Zhang, and R. D. Averitt, J. Phys. D **41**, 232004 (2008).
10. Z. Chen, R. Mohsen, Y. Gong, T. C. Chong, and M. Hong, Adv. Mater. **24**, OP143 (2012).
11. S. Lee, S. Kim, T.-T. Kim, Y. Kim, M. Choi, S. H. Lee, J.-Y. Kim, and B. Min, Adv. Mater. **24**, 3491 (2012).
12. J. Li, C. M. Shah, W. Withayachumnankul, B. S.-Y. Ung, A. Mitchell, S. Sriram, M. Bhaskaran, S. Chang, and D. Abbott, Appl. Phys. Lett. **102**, 121101 (2013).
13. I. A. I. Al-Naib, C. Jansen, N. Born, and M. Koch, Appl. Phys. Lett. **98**, 091107 (2011).